Emergence of highly coherent two-level systems in a noisy and dense quantum network

In the format provided by the authors and unedited

Supplementary Information to
Emergence of highly coherent two-level systems in a noisy and dense quantum network

1 Outline

In this supplement to Ref. [1], we provide detailed derivations of the theoretical model used to describe and analyse the spin-echo decay. In Sec. 2, we first derive the ring-exchange dephasing. In Sec. 3 we then briefly derive the algebraic decay of Rabi oscillations in pairs, as observed in Fig. 4b of the main text. The central part of this supplemental text is contained in Sec. 4, where we give more detailed derivations of the coherence-limiting mechanisms observed in the experiments. Its main results are summarized in the Methods section of the main text. Here we first discuss echo decay due to dipolar excitation hopping between Tb^{3+} ions (Sec. 4.1), pure dephasing due to magnetic dipolar and ring-exchange interactions between the Tb^{3+} ions (Sec. 4.2, as well as dephasing due to the host's nuclear spins (Sec. 4.4). Having derived these dephasing mechanisms, we explain why pairs of spins in densely doped materials, rather than single ions in a dilute sample, optimize the abundance of qubits of a certain targeted coherence (Sec. 4.4). Finally, we fit all our experimental data to the derived analytical/numerical model and present the resulting plots and parameters in Sec. 5.

2 Ring-exchange interaction

In this section we derive the ring-exchange interaction between a pair of Tb^{3+} ions and a third ion using second-order perturbation theory. As a consequence of this interaction, the transition energy for an excitation of the pair depends on the state of the neighboring ion. We refer to this self-energy-like correction as a 'ring-exchange', as it arises from a virtual exchange of excitations between the three ions.

For simplicity, we focus on clock-state ions and neglect internal dipolar fields, setting $h_i = 0$. The Hamiltonian of three clock-state ions in the secular approximation reads

$$\mathcal{H} = \frac{1}{2}\sum_{i=1}^{3}\Delta_i \tau_i^x + \left(J_{\text{pair}}\tau_1^+\tau_2^- + J_{13}\tau_1^+\tau_3^- + J_{23}\tau_2^+\tau_3^- + h.c.\right), \tag{1}$$

with the Pauli matrices τ^x and $\tau^\pm \equiv (\tau^z \mp i\tau^y)/2$ acting in the basis of the single-ion eigenstates. The ions 1 and 2 that form the pair are assumed to be resonantly coupled, i.e., $|J_{\text{pair}}| \gg \frac{1}{2}|\Delta_1 - \Delta_2|$, and more strongly coupled to each other than to the third ion, $|J_{13}| \approx |J_{23}| \ll |J_{\text{pair}}|$. We treat the couplings J_{13}, J_{23} in second-order perturbation theory. The energies for the pair transitions $|01 + 10\rangle \to |00\rangle, |11\rangle$ depend on the state $s \in [0,1]$ of the third ion, and the pair transition energies $|01 + 10\rangle \to |\tau\tau\rangle$ (with $\tau \in \{0,1\}$) are found to differ by[1]

$$V_{\text{ring}} \equiv \frac{1}{4}\left(|\varepsilon_{01+10,1} - \varepsilon_{\tau\tau,1}| - |\varepsilon_{01+10,0} - \varepsilon_{\tau\tau,0}|\right) = (1 - 2\tau)\frac{J_{13}J_{23}}{2[(\Delta_{\text{pair}} - (1 - 2\tau)J_{\text{pair}}) - \Delta_3]}. \tag{2}$$

Note that the denominator contains the detuning between the frequency of the single ion, Δ_3, and the energy difference $|\varepsilon_{01+10} - \varepsilon_{1-\tau,1-\tau}|$ between $|01 + 10\rangle$ and the pair state $|1 - \tau, 1 - \tau\rangle$ that is *not* involved in the probed transition. For dipolar interactions $J \propto r^{-3}$, the ring-exchange decays as $V_{\text{ring}}(r) \propto r^{-6}$ with the distance r between pair and single ion.

The above derivation (2) is only slightly modified in the case of a virtual exchange of an excitation between a clock-state pair and a third ion in a different hyperfine state. One simply has to

---

[1]The factor 4 is owed to the fact that a pair and a single ion, described as effective spins $\sigma_{1,2}$ and Hamiltonian $H_{\text{int}} = V\sigma_1^z\sigma_2^z$, come with energy differences $(\epsilon_{1,1} - \epsilon_{-1,1}) - (\epsilon_{1,-1} - \epsilon_{-1,-1}) = 4V$

replace the transition frequency of the third ion, Δ_3, and take into account the off-diagonal matrix elements $m_{\text{off}}(I^z) = \Delta/\sqrt{\Delta^2 + h^2(I^z)}$ of the corresponding hyperfine state in the dipolar interaction, J_{13}, J_{23}. The dephasing resulting from ring-exchange is discussed in Sec. 4.2.

We also note that the derivation of the ring-exchange can be seen as the leading term of a virial expansion, which is an expansion at low density. There are corrections involving few (> 3)-body interactions which eventually kick in at high enough density $x = O(1)$, where typical distances are of the order of the lattice constant. At low density, a pair is instead correctly described as interacting separately with every one of its (typically single ion) neighbors.

3   *nnn* pair spin-echo: Algebraic decay

Here we derive the algebraic decay of the Rabi oscillations of *nnn* pairs as observed in Fig. 4b of the main text. The pulse scheme involves a first pulse of length t_p with frequency $\omega_p \approx \Delta - J_{\text{nnn}}$ and, after a waiting time τ, a second π-pulse (approximated as instantaneous). The echo is detected after another waiting time τ. We assume the inhomogeneous broadening of the pair excitations $\omega = \omega_p + \delta\omega$ to be a Gaussian $\rho_{\text{pair}}(\omega_p + \delta\omega) = \exp\left(-\frac{\delta\omega^2}{2W_{\text{pair}}^2}\right)/\sqrt{2\pi W_{\text{pair}}^2}$ centered around ω_p with standard deviation W_{pair}. Within the rotating-wave approximation, the echo then takes the form

$$I(t_p) = \int \mathrm{d}\delta\omega \, \frac{\Omega}{\sqrt{\Omega^2 + \delta\omega^2}} \sin\left(\sqrt{\Omega^2 + \delta\omega^2}\, t_p\right) \rho_{\text{pair}}(\omega_p + \delta\omega), \tag{3}$$

where Ω is the Rabi frequency of the pair. Here we neglect decoherence, which would only manifest itself on longer time scales than were probed in the experiment of Fig. 4b.

In the limit $W_{\text{pair}}^2 t_p \gg \Omega$, only $\delta\omega$ with $\delta\omega^2 t_p/\Omega \lesssim 1$ contribute significantly, and a stationary phase approximation leads to the long time asymptotics

$$I(t_p) \approx \frac{1}{2}\sqrt{\frac{\Omega}{W_{\text{pair}}^2 t_p}} \sin(\Omega t_p + \pi/4) \propto \frac{1}{\sqrt{t_p}}, \tag{4}$$

with an algebraic decay of the Rabi oscillations.

4   Theoretical modelling of decoherence of Tb^{3+} excitations

In this section we discuss the various decoherence mechanisms for Tb^{3+} excitations with dipolar interactions. We analyze the spin echo probed at frequency ω_p after a CPMG sequence involving N short π-pulses applied at times $t = (2n-1)\tau$ ($1 \leq n \leq N$). To describe the echo decay, we take into account several decoherence mechanisms: (i) decay of excitations due to dipolar hopping, (ii) magnetic noise from other Tb^{3+} ions, (iii) ring-exchange with Tb^{3+} ions, and (iv) magnetic noise from fluorine nuclear spins. The phonon-induced relaxation rate is on the order of milliseconds and can thus be neglected in the analysis of our experiments (Supp.Fig. 1). Below, we sketch the derivation of each contribution in the high temperature limit ($T \gg \Delta$), and summarize the results that are then used to numerically fit the data. A more detailed analysis will be published elsewhere. The numerical parameters of the different dephasing sources are given in Sec. 5.

4.1   Lifetime of dilute spins in the presence of dipolar hopping

The crystal field splittings $\Delta_i = \Delta + \delta\Delta_i$ of the ions are subject to random shifts $\delta\Delta_i$. We model their distribution $\rho_\Delta(\omega)$ as Gaussian with standard deviation W_Δ. The excitation energy $\Delta E_{I_i^z} = \pm\sqrt{\Delta_i^2 + h_i^2(I_i^z)}$ with the effective longitudinal field $h_i(I_i^z) = h(I_i^z) + \delta h_i$ on a given
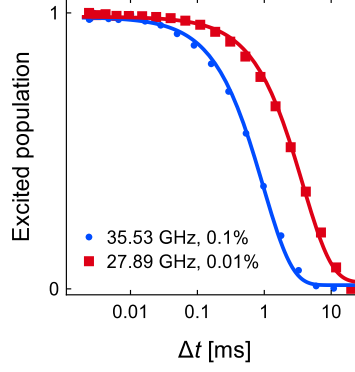
Figure 1: **Phonon relaxation times.** Comparison of T_1 relaxation times of nnn pairs at $x = 0.1\%$ (blue) to those of typical ions at $x = 0.01\%$ (red). A simple exponential fit yields T_1 times of 1.0 ms and 3.7 ms, respectively. Their ratio agrees well with the theory of decoherence by acoustic phonons, $1/T_1 \propto M^2 \omega^3$, where M is a phonon matrix element and ω is the transition frequency [2], which predicts a ratio of $2 \times (35.53/27.89)^3 = 4.1$. The phonon relaxation times are orders of magnitude longer than the relevant coherence times in the echo experiments of the main text and can thus be neglected.

site depends on the local field internal field δh_i and on the nuclear spin state I_i^z via the hyperfine interaction A, *i.e.* $h(I_i^z) = \frac{g_{\parallel} \mu_B}{2} B_z + \frac{A}{2} I_i^z$. The algebraic tail of dipolar interactions $J(\vec{r}) = J_0/r^3 (1 - 3\cos^2 \theta)$, with $J_0 = \mu_0 (\mu_B g_{\parallel}/2)^2/(4\pi)$ being the dipolar interaction constant, assures that a given Tb^{3+} excitation can always find resonant sites with energy mismatch smaller than the hopping amplitude $J_{ij} = J(\vec{r}_{ij}) m_{\text{off}}(I_i^z) m_{\text{off}}(I_i^z)$,

$$|\Delta E_{I_i^z} - \Delta E_{I_j^z}| \leq 2c_{\text{res}} |J_{ij}|, \tag{5}$$

where the numerical factor $c_{\text{res}} = O(1)$ defines a precise resonance condition and the hopping matrix element for hyperfine state I^z is $m_{\text{off}}(I^z) = \Delta/\sqrt{\Delta^2 + h^2(I^z)}$. Due to the smallness of the dipolar interaction, such excitation hopping can only be resonant between Tb^{3+} ions in the same nuclear-spin state. Their effective concentration is $x_{\text{eff}} = x/(2I+1) = x/4$, corresponding to a spatial density $n = 4x_{\text{eff}}/(a^2 c)$.

We focus below on the lifetime of clock-state excitations with $m_{\text{off}}(I^z) = 1$, neglecting weak internal fields. The derivation also carries over to magnetized hyperfine states, modulo modified hopping matrix elements and diagonal matrix elements $m(I^z) = |h(I^z)|/\sqrt{\Delta^2 + h^2(I^z)}$, which modify the disorder strength according to $W_{I^z} \approx \sqrt{W_\Delta^2 + \langle \delta h_i^2 \rangle m^2(I^z)}$. In the derivations, we consider excitation frequencies in different ranges to differentiate between 'single ions' and pairs. The detuning of the probed frequency ω_p from the mean CF energy Δ is denoted by $\Delta \omega_p \equiv \omega_p - \Delta$.

4.1.1 Decay of excitations of typical single clock-state ions ($|\Delta \omega_p| \lesssim W_\Delta$)

We first consider the effect of resonant hopping on the lifetime of typical clock-state ions with excitation energy in the middle of the spectrum of inhomogeneously broadened CF energies, $|\Delta \omega_p| \lesssim W_\Delta$. Such typical ions have no atypically close neighbors, since the dipolar interaction with them would imply a significant shift in $|\Delta \omega_p|$. We thus refer to these spins as 'single ions' (to distinguish them from ion pairs or larger ion clusters).

The typical decay time is found by counting the number of resonant sites $N(J)$ having interactions exceeding J and satisfying the resonance condition of Eq. (5). The lifetime τ_s of typical single ions is of the order of the inverse interaction strength with their nearest resonant neighbor. The associated energy scale J_{res} is found from $N(J_{\text{res}}) = c_N$ with $c_N = O(2)$. The

3

frequency-dependent typical spin-flip rate is obtained as

$$\frac{1}{\tau_s(\omega_p)} = 2c_\tau |J_{\text{res}}(\omega_p)| = \frac{2ec_\tau}{c_{\text{res}}}\frac{J_{\text{typ}}}{\alpha(\omega_p)}\exp\left[-\frac{c_N}{c_{\text{res}}}\frac{1}{\alpha(\omega_p)}\right]. \tag{6}$$

The numerical factor c_τ relates resonant coupling and decay rate, $c_\tau \equiv 2|J_{\text{res}}(\omega_p)|\tau_s(\omega_p) = O(1)$.[2] The frequency-dependent disorder parameter $\alpha(\omega_p)$ is defined as

$$\alpha(\omega_p) = 4J_{\text{typ}}\rho_\Delta(\omega_p), \tag{7}$$

with J_{typ} the dipolar hopping between a typical site and its most strongly coupled neighbor,

$$J_{\text{typ}} \equiv \frac{8\pi}{9\sqrt{3}}nJ_0. \tag{8}$$

Equation (6) holds for relatively strong disorder, $\alpha(\omega_p) \leq c_N/c_{\text{res}}$. In the method section of the main text, we abbreviate $c_1 = c_{\text{res}}/c_N$ and $c_2 = c_\tau/c_{\text{res}}$.

The decoherence due to excitation hopping dominates the Hahn-echo decay of clock-ions in the range $|\Delta\omega_p| \lesssim W_\Delta$ at short times $t \ll \tau_s(\omega_p)$ where it results in a simple exponential decay

$$I_{\text{dec,single}}(t \ll \tau_s(\omega_p)) = e^{-t/\tau_s(\omega_p)}. \tag{9}$$

These times are, however, too short to be measured in our experimental set-up.

4.1.2 Decay of rare single-ion clock-states ($|\Delta\omega_p| \lesssim W_\Delta$) with atypically distant neighbors

Echo contributions from typical clock ions decay exponentially for $t \gg \tau_s(\omega_p)$. In that regime, the echo signal is instead dominated by rare, long-lived spins, whose nearest resonant site is atypically far away. With high probability, the nearest resonant site is a typical site, with closer resonant neighbors. Thus, the hopping to that site is generally much slower than the subsequent hopping away from that site. The isolated site can thus be treated as being coupled to an energy-continuum of lifetime-broadened typical sites, and the decay rate can be calculated with Fermi's golden rule, similarly as in Ref. [3]. Assuming the same lifetime $\tau_s \equiv \tau_s(\omega = \Delta)$ [Eq. (6)] for all neighboring sites, each contributes to the total decay rate with a partial rate

$$\gamma_i \equiv \gamma(r_i, \theta_i, \Delta_i) \approx \frac{1}{2}2\pi\left(\frac{J_0}{r_i^3}(1 - 3\cos^2\theta_i)\right)^2\mathcal{A}(\omega_p;\Delta_i), \tag{10}$$

where $\mathcal{A}(\omega_p;\omega) = \frac{1}{\pi}\frac{1/(2\tau_s)}{1/(2\tau_s)^2 + (\omega - \omega_p)^2}$ is the Lorentzian broadened density of states at energy ω_p. Accounting for the random spatial distribution of Tb^{3+} ions, one obtains a distribution $p(\gamma = \sum_i \gamma_i) = e^{-1/(4\gamma T_1(\omega_p))}/\sqrt{4\pi\gamma^3 T_1(\omega_p)}$ of decay rates, from which one can compute the sample averaged echo signal (for $t \gg \tau_s$)

$$I_{\text{dec,single}}(t \gg \tau_s(\omega_p)) = \int_0^\infty d\gamma\, p(\gamma)e^{-\gamma t} = \exp\left[-\sqrt{\frac{t}{T_1(\omega_p)}}\right], \tag{11}$$

where the frequency-dependent lifetime $T_1(\omega_p)$,

$$\frac{1}{T_1(\omega_p)} = 4\pi^2 J_{\text{typ}}^2\left[\int d\omega\, \rho_\Delta(\omega)\, \mathcal{A}^{1/2}(\omega_p;\omega)\right]^2, \tag{12}$$

---

[2] A self-consistent estimate based on Fermi's golden rule yields $\tau_s^{-1}(\omega_p) = 2|J_{\text{res}}(\omega_p)|$. Shortcomings of this approximation are captured by the deviation of the coefficient c_τ from 1.

scales roughly as $\frac{1}{T_1(\omega_p)} \approx \frac{\pi}{2} \frac{1}{\tau_s} \left(\frac{\rho_\Delta(\omega_p)}{\rho_\Delta(\Delta)} \right)^2$ for large disorder, as long as $\rho_\Delta(\omega_p)/\rho_\Delta(\Delta)$ is not exponentially small. For a general disorder distribution $\rho_\Delta(\omega)$, it has to be evaluated numerically. For our fits we model the crossover from short times (9) to long times (11) by a simple interpolating function,

$$I_{\text{dec,single}}(t) = \exp \left[-\frac{\left(\frac{t}{\tau_s(\omega_p)} \right)}{\left(1 + \left(\frac{t}{\tau_s(\omega_p)} \right) \left(\frac{T_1(\omega_p)}{t} \right)^{1/2} \right)} \right]. \tag{13}$$

4.1.3 Decay of excitations of pairs of clock-states ($|\Delta\omega_p| \gtrsim W_\Delta$)

At detunings $|\Delta\omega_p| \gtrsim W_\Delta$, the signal is dominated by compact pairs of (clock-state) Tb^{3+} whose dipolar interaction shifts the excitation energies, *cf.* Fig. 2a of the main text. For those, resonant hopping to equivalent pairs is negligible, since their concentration and thus their dipolar coupling scales as $\sim x^2 \ll 1$. Excitations on such pairs will instead predominantly decay to non-resonant single ions, as allowed by the lifetime-broadening of the latter. The decay follows from Fermi's golden rule (10) as in the preceding subsection, with only two small differences: (i) The hopping matrix element is enhanced by a factor of $\sqrt{2}$, leading to an additional factor of 2 in the expression for the hopping rate. (ii) A pair realizes an effective three-level system with the symmetric states $|00\rangle$, $|01 + 10\rangle$, and $|11\rangle$, creating an additional hopping channel. Taking both factors into account, we find the spin-echo decay of pairs due to the finite lifetime as

$$I_{\text{dec,pair}}(t) = \int_0^\infty d\gamma \, p(\gamma) e^{-3\gamma t} = \exp \left[-\sqrt{\frac{t}{T_{1,\text{pair}}(\omega_p)}} \right], \tag{14}$$

with the same $p(\gamma)$ as before. The life time $T_{1,\text{pair}}(\omega_p)$ is three times smaller than that of (the very rare) single ions with the same excitation frequency, *cf.* Eq. (12),

$$\frac{1}{T_{1,\text{pair}}(\omega_p)} = 12\pi^2 J_{\text{typ}}^2 \left\langle \sqrt{\mathcal{A}(\omega_p; \omega)} \right\rangle^2 \approx 12\pi^2 J_{\text{typ}}^2 \mathcal{A}(\omega_p; \Delta) \approx 6\pi \left(\frac{J_{\text{typ}}}{\Delta\omega_p} \right)^2 \frac{1}{\tau_s}. \tag{15}$$

Note that, in contrast to the single ions (13), there is no crossover from a short- to a long-time regime for the decay of pairs. Indeed, the short-time regime becomes irrelevant at large detunings for which $\tau_s(\omega_p) \gg T_{1,\text{pair}}(\omega_p)$.

4.2 Pure dephasing from dilute spins with dipolar interactions

Apart from inducing finite lifetimes, the dipolar interactions also lead to pure dephasing (T_2). Below we discuss the decoherence of a two-level systems (TLS) for the case that it is dominated by interactions with dilute neighboring (Tb^{3+}) fluctuators. We discuss couplings that decay as general power laws of the distance r, $V(r) \sim r^{-\gamma}$. This covers both magnetic noise between magnetic moments of the TLS and fluctuators ($\gamma = 3$) as well as dephasing of barely magnetized clock-state pairs via ring-exchange ($\gamma = 6$). Note that even for clock states the former does not vanish completely, as small residual moments are induced by internal magnetic fields from the fluorine ions.

We consider a spin or spin pair as the TLS of interest and model all Tb^{3+} ions as classical random fluctuators which flip stochastically between $s_j(t) = \pm 1$ with rate κ. Since the dephasing factors from independent sources simply multiply, it suffices to analyze the fluctuators belonging to a single hyperfine state I^z. We further assume that the corresponding ions all have the same (I^z-dependent) fluctuation rate κ and flip independently from each other. To simplify the analysis, we treat a simple power law interaction, $V(\vec{r}) = V_0^{(\gamma)} g_\gamma(\theta)/r^\gamma$, which depends on the distance r and the angle θ between $\vec{r}$ and the crystallographic c-direction via a dimensionless function $g_\gamma(\theta)$. For the ring-exchange interaction, we define $g_{\gamma=6}(\theta) = (1 - 3\cos^2\theta)^2$ and

$V_0^{(\gamma=6)} = J_0^2/(2\Delta\omega)$, with $\Delta\omega = \Delta - \Delta\omega_p - \Delta E_{I^z}$ the mismatch between the neighbor's excitation energy ΔE_{I^z} and $\Delta - \Delta\omega_p$, the pair's transition energy that is not driven. For the residual magnetic interactions, we use $V_0^{(\gamma=3)} = J_0 m_p m(I^z)$, where m_p is a typical fluorine-induced moment and $m(I^z)$ is the moment of the neighboring fluctuator, and we define $g_{\gamma=3}(\theta) = 1 - 3\cos^2\theta$. In the continuum limit, similarly as was done in Ref. [4] for the Hahn-echo sequence ($N = 1$) with dipolar interactions ($\gamma = 3$), one can integrate over the distribution of fluctuator positions, leading to the analytic expression of the echo-decay function

$$I(t) = \exp\left[-[\bar{V}(\gamma)]^{3/\gamma} G_\gamma(t)\right], \tag{16}$$

where

$$\bar{V}(\gamma) \equiv 2V_0^{(\gamma)} \left[\cos\left(\frac{3\pi}{2\gamma}\right) \left|\Gamma\left(-\frac{3}{\gamma}\right)\right| \frac{4\pi}{\gamma} n \left(\int_{-1}^{1} \frac{d(\cos(\theta))}{2} |g_\gamma(\theta)|^{3/\gamma}\right)\right]^{\gamma/3}, \tag{17}$$

is a typical nearest neighbor interaction, Γ being the Euler Gamma function. The factor $G_\gamma(t)$ is the following average over spin-flip histories (denoted by $\langle.\rangle_s$)

$$G_\gamma(t) \equiv \left\langle \left|\int_0^t s(t')f(t')dt'\right|^{3/\gamma}\right\rangle_s, \tag{18}$$

whereby the function $f(t') = \sum_{i=0}^{N}(-1)^i \left[\theta(t' - [2i-1]\tau) - \theta(t' - [2i+1]\tau)\right]$ describes the alternating spin orientation of the TLS ($f(t') = \pm 1$) as imposed by the CPMG sequence of π-pulses. Below we give approximations of $G_\gamma(t)$ for short times ($\kappa t \ll 1$) and long times ($\kappa t \gg N$).

4.2.1 Short-time regime $\kappa t \ll 1$

First we consider the short-time regime $\kappa t \ll 1$. The echo is diminished only if any spin flips occur at all (since for constant $s(t')$ one finds $\int_0^t s(t')f(t')dt' = 0$). From events with one spin flip, one easily finds that $G_\gamma(t) \sim \kappa t(t/N)^{3/\gamma}$. Following Ref. [4], the spin-echo intensity for short times $\kappa t \ll 1$ is obtained fully quantitatively as

$$I(t \ll 1/\kappa) = \exp\left[-\left(\frac{t}{T_s}\right)^{1+3/\gamma}\right], \tag{19}$$

with the short-time timescale

$$\frac{1}{T_s} = \frac{1}{N^{3/(3+\gamma)}} \left(\frac{\gamma}{3+\gamma}\kappa\bar{V}^{3/\gamma}(\gamma)\right)^{\gamma/(3+\gamma)}. \tag{20}$$

The stretched exponential reflects the temporal growth of the range over which the interactions have a detrimental effect, when a neighboring spin flips.

For magnetic Tb^{3+} ions with dipolar interactions ($\gamma = 3$), or for ring-exchange of pairs ($\gamma = 6$), we find, respectively, the short-time echo decay

$$I_{\mathrm{magn}}(t \ll 1/\kappa) = \exp\left[-\left(\frac{t}{T_{\mathrm{magn},s}}\right)^2\right],$$

$$\frac{1}{T_{\mathrm{magn},s}} = \left(\frac{\kappa}{2}\frac{\bar{V}^{(\gamma=3)}}{N}\right)^{1/2} \approx 2.25 \left(\frac{\kappa V_0^{(\gamma=3)} n}{N}\right)^{1/2},$$

$$I_{\mathrm{ring}}(t \ll 1/\kappa) = \exp\left[-\left(\frac{t}{T_{\mathrm{ring},s}}\right)^{3/2}\right],$$

$$\frac{1}{T_{\mathrm{ring},s}} = \left(\frac{2\kappa}{3}\sqrt{\frac{\bar{V}^{(\gamma=6)}}{N}}\right)^{2/3} \approx 2.44 \left(\frac{\kappa^2 V_0^{(\gamma=6)} n^2}{N}\right)^{1/3}. \tag{21}$$

4.2.2 Long-time regime $\kappa t \gg N$

In the long-time regime $\kappa t \gg N$, each spin flips many times between two consecutive pulses in the CPMG sequence. Since the π-pulses are only effective in cancelling noise contributions at frequencies lower than $1/\tau = N/t$, the only remaining effect of the CPMG sequence lies in the cancellation of static fields. As far as noise from fluctuators is concerned, its contribution to echo signal suppression is essentially independent of N in this regime.

Instead of directly evaluating $G_\gamma(t)$ in the long-time regime, as was *e.g.* done in Ref. [4] for $\gamma = 3$, we proceed in a different way. At times $\kappa t \gg N$, merely TLS's that couple only to 'weak fluctuators' (defined by $V_j \ll \kappa$) contribute to the echo, since TLS's coupled to strong fluctuators ($V_j \gg \kappa$) will already have decohered. A single weak fluctuator i leads to an exponential spin-echo decay $\exp(-\gamma_i t)$ with the motionally narrowed decoherence rate $\gamma_i = 2V_i^2/\kappa$ [5]. Similarly as in the derivation of Eq. (11), we can then derive a distribution $p(\gamma = \sum_i \gamma_i)$ of the total dephasing rate. Following the same steps, we find at long times $\kappa t \gg N$

$$I(t \gg N/\kappa) = \exp\left[-\left(\frac{t}{T_l}\right)^{3/(2\gamma)}\right], \tag{22}$$

with the timescale

$$\frac{1}{T_l} = \left(\frac{\sqrt{\pi}}{\Gamma\left(\frac{\gamma-3}{2\gamma}\right)\cos\left(\frac{3\pi}{2\gamma}\right)}\right)^{2\gamma/3}\frac{2\bar{V}^2(\gamma)}{\kappa}. \tag{23}$$

For magnetic Tb^{3+} ions with dipolar interactions ($\gamma = 3$) and ring-exchange of pairs ($\gamma = 6$), we find, respectively, the long-time asymptotics

$$I_{\text{magn}}(t \gg N/\kappa) = \exp\left[-\left(\frac{t}{T_{\text{magn,l}}}\right)^{1/2}\right], \quad \frac{1}{T_{\text{magn,l}}} = \frac{2}{\pi}\frac{\left(\bar{V}^{(\gamma=3)}\right)^2}{\kappa} \approx 65.3\frac{\left(V_0^{(\gamma=3)}n\right)^2}{\kappa},$$

$$I_{\text{ring}}(t \gg N/\kappa) = \exp\left[-\left(\frac{t}{T_{\text{ring,l}}}\right)^{1/4}\right], \quad \frac{1}{T_{\text{ring,l}}} \approx 0.46\frac{\left(\bar{V}^{(\gamma=6)}\right)^2}{\kappa} \approx 488\frac{\left(V_0^{(\gamma=6)}n^2\right)^2}{\kappa}. \tag{24}$$

4.2.3 Crossover from short to long times

Above we have derived the asymptotics of spin echos under the CPMG sequence for short (21) and long times (24). To conveniently fit the experimental data at all times, we interpolate between them with a form that comes as a close as possible to an exact evaluation of the dephasing function (16). For ring-exchange noise of pairs ($\gamma = 6$) we use

$$I_{\text{ring}}(t) = \exp\left[-\frac{\left(\frac{t}{T_{\text{ring,s}}}\right)^{3/2}}{\left(1 + \left(\frac{t}{T_{\text{ring,s}}}\right)^{3\beta/2}\left(\frac{T_{\text{ring,l}}}{t}\right)^{\beta/4}\right)^{1/\beta}}\right]. \tag{25}$$

where the parameter β tunes the sharpness of the crossover and is fit to the numerically evaluated analytic expression of the echo decay. Since the crossover function is an approximation to the analytical result, the fitted tuning parameter β depends weakly on the evaluated time-window. We used $0 \le t \le 20/\kappa$ and found $\beta \approx [1.2, 1.1, 1.1, 1.0, 0.93]$ for $N = [1, 2, 3, 4, 5]$. The systematic decrease of β with N correctly reflects that the crossover from short to long times becomes longer with increasing N.

For magnetic noise ($\gamma = 3$), Hu and Hartmann [4] had derived an analytic expression for the Hahn-Echo ($N = 1$), which is, however, unsuitable for numerical evaluation at long times $\kappa t \gg 1$.

To cover long times and general N, we resort also here to using a phenomenological crossover function

$$I_{\mathrm{magn}}(t) = \exp\left[-\frac{\left(\frac{t}{T_{\mathrm{magn,s}}}\right)^2}{\left[1 + \left(\frac{t}{T_{\mathrm{magn,s}}}\right)^{2\beta}\left(\frac{T_{\mathrm{magn,l}}}{t}\right)^{\beta/2}\right]^{1/\beta}}\right],\tag{26}$$

with $\beta \approx [0.93, 0.74, 0.63, 0.58, 0.54]$ obtained for $N = [1, 2, 3, 4, 5]$ from fitting to the exact analytical function in the window $0 \le t \le 20/\kappa$.

4.3 Dephasing due to the host's nuclear spins (fluorine noise)

TLS's with a sizeable magnetic moment create an inhomogeneous dipolar field around themselves. This suppresses resonant flip-flops between nuclear spins and induces a so-called 'frozen core' of nuclear spins. [6][7, 8]. The main dephasing is then contributed by the many nuclear spins at the boundary of this frozen core. However, clock states have only very small residual magnetic moments (mostly induced by fluorine fields), and thus the frozen core barely exists. The dipolar field of clock states only slows the dynamics of the nearest fluorine spins. As a result the dephasing is still dominated by the most strongly coupled (i.e., the nn and nnn) fluorine, which, however, fluctuate at a lower rate than the fluorine further away.

As a (nn or nnn) fluorine spin flips, the longitudinal fields on a nearby Tb^{3+} changes – mediated by the effective interaction $J_{\parallel}(\vec{r}_i) = \mu_0\mu_F(\mu_B g/2)/(4\pi r_i^3)(1 - 3\cos^2\theta_i)m_p$ (μ_F being the fluorine moment). This rapidly dephases the TLS, since the coupling is much larger than the fluorine's fluctuation rate, $J_{\parallel}(\vec{r}_i) \gg \kappa_i$. A single strongly coupled fluctuator i leads to the Hahn-echo decay (for $N = 1$ π-pulses) [5]

$$I_i(t) = \frac{e^{-\kappa_i t}}{2\lambda}\left[(\lambda + 1)e^{\kappa_i\lambda t} + (\lambda - 1)e^{-\kappa_i\lambda t}\right] \approx e^{-\kappa_i t}\left(1 + \frac{\kappa_i}{2J_{\parallel}(\vec{r}_i)}\sin\left[2J_{\parallel}(\vec{r}_i)t\right]\right),\tag{27}$$

with $\lambda \equiv \sqrt{1 - [2J_{\parallel}(\vec{r}_i)/\kappa_i]^2}$. To describe the effect of all nn and nnn fluorine neighbors, we multiply their echo shape, approximating their fluctuations as uncorrelated.

In Eq. (27), the clock states are assumed to have a small, but constant moment of a typical magnitude m_p. However, in reality the moment is induced by the fluorine neighborhood and thus differs from ion to ion. Accordingly, the decay function should be appropriately averaged over the distribution of couplings.[3] The couplings are expected to have a standard deviation of the order of the typical $J_{\parallel}$, and thus the oscillatory terms average out on a time scale $\gtrsim 1/J_{\parallel}$. We capture this effect qualitatively by assuming a typical moment and associated couplings $J_{\parallel}(\vec{r}_i)$, but we retain the oscillatory term in $I_i(t)$ only up to $t \le t_c = \pi/(2J_{\parallel}(\vec{r}_i))$ and drop it for longer times, setting

$$I_{F,nnn}(t) = \prod_{i\in\{nn,nnn\}} \tilde{I}_i(t), \quad \text{with } \tilde{I}_i(t) = \begin{cases} I_i(t), & \text{for } t < \frac{\pi}{2J_{\parallel}(\vec{r}_i)}, \\ e^{-\kappa_i t}, & \text{for } t \ge \frac{\pi}{2J_{\parallel}(\vec{r}_i)}. \end{cases}\tag{28}$$

To generalize the decay function to a CPMG sequence with $N > 1$ pulses, we observe that the echo at short times is $I_{F,nnn}(t) \sim \sum_i \kappa_i t(J_{\parallel}\tau)^2 \sim \sum_i \kappa_i(J_{\parallel}/N)^2 t^3$, where N essentially just renormalizes the couplings, $J_{\parallel} \to J_{\parallel}/N$ (Ext.Dat.Fig. 3). This also holds for the function (27) up to times $tJ_{\parallel} \ll N$, while at longer times dephasing is unaffected by N and independent of $J_{\parallel}$. Thus both limits of the echo suppression due to fluorine under a CPMG sequence are still well described by Eq. (28), provided all couplings are divided by N. This observation suggests that

---

[3]If the moments were static in time, the echo would receive larger contributions from very small moments. However, the moments themselves evolve as neighboring spins flip, so that atypically small moments do not survive for long.

we extend this recipe to intermediate times, too, in order to obtain a reasonable approximation for that time regime. The resulting function is used in the numerics to describe the CPMG data of the nnn pair, since its echo is dominated by fluorine noise. At short times, we find that the coherence time scales as $T_{\text{char}} \propto N^{2/3}$, the same scaling as observed in the CPMG data (Fig. 4c). At long times, the decay function asymptotes to a simple exponential with timescale $T_{F,nnn} = 1/(16\kappa_F)$ (since there are 16 strongly coupled neighboring fluorine ions).

Since typical magnetic moments of a nnn pair are smaller than those of looser pairs (due to corrections of order J_{pair}/Δ which are sizable for the strongly coupled nnn pair), we cannot use the same fitting parameters to describe the coupling of looser pairs to fluorine. For looser pairs, fluorine only plays a role in the long-time regime of the decay, short times being dominated by ring-exchange. Thus, a fit cannot capture the short-time regime of Eq. (28) very well. We therefore only aim at fitting the long-time decay. We make the phenomenological ansatz of a stretched exponential which allows us to capture part of the crossover from the short-time regime as well,

$$I_F = \exp\left[-(t/T_F)^{\beta_F}\right]. \tag{29}$$

Here we take T_F and β_F as free fit parameters independent of the probe frequency ω_p, anticipating an exponent β_F close to 1.

4.4 Optimizing the abundance of coherent qubits

In a host containing nuclear spins, the coherence of qubits is ultimately bounded from above by the magnetic noise of those spins. In a nuclear-spin free host, however, dephasing of clock state ions will be limited only by excitation hopping and/or ring-exchange fluctuations.

The relative disorder strength seen by single ions remains moderate with increasing dilution if we assume that disorder is dominated by strain from the dopants and thus scales as x, in the same way as the dipolar couplings among dopants. Therefore single ions flip with a rate proportional to the typical dipolar interactions, *i.e.* $\kappa_s \sim x$ (Eq. (6)).

In contrast, pairs dephase predominantly due to ring-exchange with their closest clock state neighbors. That interaction scales as $V_{\text{ring}} \sim J_{\text{typ}}^2 \sim x^2$ (Eq. (2)). For strong dilution the corresponding dephasing is in the motionally narrowed regime (since $V_{\text{ring}} \ll \kappa_s$), which leads to very slow typical dephasing rates scaling as $1/\tau_{\text{pair}} \sim V_{\text{ring}}^2/\kappa_s \sim x^3$ (Eq. (24)).

These considerations imply that a sample where almost all ions have a coherence time $\geq T_2$ requires a dilution $x \sim 1/T_2$, whereas a sample with higher concentration $x' \sim 1/T_2^{1/3}$ hosts a larger density $\sim (x')^2 \sim 1/T_2^{2/3}(\gg 1/T_2 \sim x)$ of pairs with equally long coherence time. We thus reach the conclusion that to maximize the density of coherent qubits in a randomly doped magnet, it is best to focus on pairs in high density samples, rather than to increase the dilution such that all typical ions reach the desired degree of coherence.

5 Numerical fit of data to the theory

We now combine the different dephasing mechanisms discussed above to obtain a full model that we use to simultaneously fit all the experimental echo data for the various frequencies and different echo protocols. The fitting function and the detailed fitting procedure are outlined in the method section of the main text. The fit parameters that we need to determine are: The numerical coefficients c_1, c_2 appearing in the fluctuation rate of spins, Eq. (6), the spread of CF splittings W_Δ of single ions, the effective fluorine dephasing parameters of loose pairs (β_F,T_F), the coupling parameters of the nnn Tb pair to nearby fluorine spins ($J_\|(\vec{r}_{nn})$ and the fluctuation rate κ_F of the latter). Knowing the parameters c_1, c_2 and W_Δ allows us to calculate the Tb^{3+} fluctuation rates κ_{I^z} for all hyperfine states at any concentration (assuming that disorder in

I^z	$\hbar/\bar{V}$			
	loose pair		nnn pair	
	magnetic ($\gamma = 3$)	ring-exchange ($\gamma = 6$)	magnetic ($\gamma = 3$)	ring-exchange ($\gamma = 6$)
$-3/2$	$1.2\,\mathrm{ms}$	$0.4\,\mu\mathrm{s}$	$1.9\,\mathrm{ms}$	$8.4\,\mu\mathrm{s}$
$-1/2$	$12.7\,\mu\mathrm{s}$	$0.2\,\mu\mathrm{s}$	$21\,\mu\mathrm{s}$	$9.6\,\mu\mathrm{s}$
$+1/2$	$6.9\,\mu\mathrm{s}$	$2.2\,\mu\mathrm{s}$	$11\,\mu\mathrm{s}$	$13.6\,\mu\mathrm{s}$
$+3/2$	$5.1\,\mu\mathrm{s}$	$6.4\,\mu\mathrm{s}$	$8.4\,\mu\mathrm{s}$	$21.3\,\mu\mathrm{s}$

Table 1: Typical inverse interaction strengths $\bar{V}$ (Eq. 17) at Tb^{3+} concentration $x = 0.1\%$ for a weak clock-state pair (detuning frequency $\Delta\omega = 2\pi \times -0.5\,\mathrm{GHz}$, corresponding to 2-3 lattice spacings between the Tb^{3+}) and for the nnn clock-state pair (detuning $\Delta\omega = 2\pi \times 7.61\,\mathrm{GHz}$) with neighboring Tb^{3+} in various hyperfine states labelled by I^z. $\gamma = 3, 6$ refers to the exponent governing the spatial decay of the interactions. For the loose pair, the by far most strongly coupled Tb^{3+} ions are single clock state ions ($I_z = -3/2$) and those with similar nuclear spin, $I_z = -1/2$. Ring-exchange is seen to be the dominant interaction, except for the most strongly magnetized HF species ($I^z = 3/2$), for which both interactions are weak, however. For the nnn pair, all interactions are weak. Ring-exchange dominates for the hyperfine states $I_z = -3/2$, $I_z = -1/2$, while magnetic interactions dominate for neighbors having $I_z = 1/2$, $I_z = 3/2$. The latter interactions leave no visible trace in the experimental echo decay though due to the exponentially slow flip rates of these states (Table 2).

the CF splittings is dominated by elastic strain due to the random doping, and thus $W_\Delta \propto x$). Below we summarize the extracted timescales and show the numerical fits.

5.1 Coupling parameters of clock-state pairs with neighboring Tb^{3+} ions

We consider clock state pairs having nuclear spin $I^z = -3/2$, with the clock field of $B_z = 38\,\mathrm{mT}$ being applied. The interaction strengths at typical nearest neighbor distance between such a pair and a single neighbor Tb^{3+} in one of four possible hyperfine states, *cf.* Eq. (17), are listed in Table. 1 for a pair with dipole-induced detuning $\Delta\omega = -2\pi \times 0.5\,\mathrm{GHz}$ and for the nnn pair ($\Delta\omega = 2\pi \times 7.61\,\mathrm{GHz}$), respectively. Magnetic interactions are estimated with a typical effective moment on the clock-state pair, which we take as the HWHM value of its (Gaussian) distribution, $\approx 0.277\,\mathrm{mT}$. The latter is induced by the distribution of fluorine magnetic fields, with the fluorine spins being aligned parallel or anti-parallel to the external field (in contrast to the magnetic hyperfine species, where nearby fluorine spins align along the stronger dipolar field of the nearby Tb^{3+} ion). Note that the typical (total) moment of the nnn pairs ($m_p = 0.00098$) is smaller by a factor of about 1.6 than that of looser pairs with smaller detuning ($m_p = 0.0016$).[4] This difference is due to corrections of order J_pair/Δ which are sizable for the strongly coupled nnn pair. As seen from Table 1, at concentration $x = 0.1\%$ the ring-exchange of loose pairs is stronger than the residual magnetic interactions (except for the weak interactions with single $I^z = +3/2$ ions), and thus they dominate the dephasing in the relevant experimental time window.

5.2 Spin flip rates of the various Tb^{3+} hyperfine states

We used the optimal fit values $c_1 = 0.41$, $c_2 = 1.67$, $W_\Delta(x = 0.1\%) = 21\,\mathrm{MHz}$ to extract the fluctuation rates of the different HF states at concentration $x = 0.01\%$ and $x = 0.1\%$, as summarized in Table 2 (see also the following subsections). Note that only the moderate flipping times of the least magnetized hyperfine species ($I^z = -1/2$) are physically relevant. The more

---

[4]We define the moment as half the difference between the moments of the upper and the lower state of the considered transition. The typical moment is determined as the HWHM of its Gaussian distribution.

I^z	$x = 0.01\%$	$x = 0.1\%$
$-3/2$	$4.6\,\mu\text{s}$	$0.45\,\mu\text{s}$
$-1/2$	$\gg 1\,\text{s}$	$12\,\mu\text{s}$
$+1/2$	$\gg 1\,\text{s}$	$0.016\,\text{s}$
$+3/2$	$\gg 1\,\text{s}$	$\gg 1\,\text{s}$

Table 2: Fluctuation times $(\kappa_{I^z}^{-1})$ of Tb^{3+} obtained from optimal fit parameters, evaluated at the two concentrations $x = 0.01\%$ and $x = 0.1\%$ (assuming $W_\Delta \propto x$). At the lower concentration, all hyperfine states except the clock states are quasi-static on the experimental timescales.

magnetized states experience strong disorder and, within the single particle-like approximation, flip exponentially slowly due to the lack of direct resonances. However, their actual flip rates are expected to be significantly enhanced by interaction effects. Indeed, sufficiently slowly decaying algebraic interactions, such as dipolar interactions, were predicted to lead to 'spectral diffusion' of local energies [9]. The latter increases the likelihood for close resonances, and thus speeds up the typical fluctuation rate significantly, especially in the presence of strong disorder and/or dilution. However, we checked that for the concentrations of our experiments, the resulting rates are still too slow for those ions to contribute significantly to dephasing. This would change at higher concentrations, where clock state pairs, used as quantum sensors for the dynamics of the surrounding dipolar coupled Tb^{3+} ions could offer a promising route to access and study the parameter dependence of the fluctuation rates and to verify the theoretical concept of interaction-enhanced transport via spectral diffusion [10].

5.3 Fluorine dephasing

The fluorine parameters obtained from our best fit are summarized in Table 3. The effective stretching exponent $\beta_F = 1.3$ describing intermediate-to-long time dephasing for loose pairs turns out to be slightly larger than 1, as anticipated. The typical decay time is found as $T_F = 10.6\,\mu\text{s}$. For the stronger nnn pair, we find the fluctuation time $1/\kappa_F = 61\,\mu\text{s}$ of single fluorine spins. Given that there are 16 strongly coupled fluorine neighbors, this leads to a long-time characteristic decay time of $T_{F,nnn} = 1/(16\kappa_F) = 3.8\,\mu\text{s}$. The two time scales reflect the difference in the magnetic moments of looser pairs and nnn pairs. These affect the strength of the frozen core and thus the fluctuation rates of the fluorine.

Parameter	Best-fit value
c_1	0.4
c_2	1.7
$W_\Delta(x = 0.1\%)$	$21\,\text{MHz}$
T_F	$10.6\,\mu\text{s}$
β_F	1.3
$T_{F,nnn} = 1/(16\kappa_F)$	$3.8\,\mu\text{s}$
$m_{p,nnn}$	0.007

Table 3: Summary of optimal fit parameters.

The fit returns a value for the typical magnetic moment m_p of the nnn clock-state pair which is about four times larger than our estimate for a typical moment induced by random nuclear polarizations of neighboring fluorine spins.[5] We attribute the larger fitted moment of pairs to

---

[5]The factor of four refers to the typical moment on *one* site in the $|01 + 10\rangle$ state, as opposed to m_p defined in Sec. 5.1 which defines a *difference* of the *total* moment. We consider the moment of the less magnetized $|01 + 10\rangle$ state. Its moment is still considerable, but smaller than that of the $|00\rangle$ state. Thus, the fluorine spins flip faster when the nnn pair is in $|01 + 10\rangle$, dominating the decoherence time of the nnn pair.

one or several of the following aspects. (i) There might be superhyperfine interactions adding to dipolar interactions which we neglected. (ii) We approximated that nearby fluorines flip stochastically, but they rather flip-flop with other fluorines, adding a geometric factor to the fluctuating field. (iii) We neglected the fluctuations of fluorine neighbors beyond nn and nnn. (iv) We approximated the pair moment as constant in time while it will in fact evolve and sometimes become atypically large. (v) Finally, there is an uncertainty in the crossover time beyond which we neglect the echo modulations in Eq. (28). We leave the determination of the cause for future studies, that could *e.g.* use a numerical cluster-correlation expansion [11] to simulate the echo decay. Although we note that the high density of fluorine ions and the long experimental timescales might pose a challenge for numerical convergence [12].

If we fit the fluorine dephasing of loose pairs with the a similar crossover function as for the nnn pair instead of using the phenomenological stretched exponential (29) (but with different coupling parameters), we similarly find an effective static moment that exceeds the static theoretical expectation, by an even slightly bigger factor. This is presumably due to similar reasons as we discussed above. These fits thus correctly reflect the larger residual moments of looser pairs as compared to the nnn pairs.

5.4 Quantitative evaluation of numerical fits

As outlined in the method section, we scan parameters c_1, c_2 and $W_\Delta(x = 0.1\%)$. Then, for each such triplet, we fit all other parameters to minimize the sum of squared residuals of all data sets *simultaneously*. In Supp.Fig. 2a we plot the best fit value $W_\Delta(x = 0.1\%)$ as a function of c_1 and c_2. Similarly, we present in Supp.Fig. 2b the sum of squared residuals of our fits as a function of c_1 and c_2. The latter plot shows a broad range of values (c_1, c_2) with similarly good fits. These two fit parameters are strongly correlated. [6] The fits become worse once the value c_1 exceeds $c_1 \gtrsim 0.6$, which would predict the magnetic hyperfine state $I^z = -1/2$ to flip too fast and thus start contributing strongly to dephasing via ring-exchange.

The best fitting values of c_1, c_2 go together with optimal values of the single ions' CF disorder that all lie in the range $15\,\mathrm{MHz} \leq W_\Delta(x = 0.1\%) \leq 30\,\mathrm{MHz}$. This is the window of values that is consistent with the disorder $W_\mathrm{pair} = (18 \pm 3)\,\mathrm{MHz}$ of nnn pair excitations, as extracted from the frequency-dependent echo data in Fig. 2 of the main text. The lower limit of $W_\Delta^\mathrm{min} = W_\mathrm{pair}$ results if one assumes that the CF level shifts $\Delta_{i,j}$ on the two pair sites are essentially identical (e.g. if they arise from strain), while the upper limit of about $W_\Delta^\mathrm{max} \approx \sqrt{2} W_\mathrm{pair}$ is expected if the two shifts are completely uncorrelated. We plot the best fit echo traces of loose pairs for $x = 0.01\%$ and $x = 0.1\%$ in Supp.Fig. 3a and Supp.Fig. 3b, respectively. In Supp.Fig. 4 we plot the fitted CPMG data for our optimal fitting parameters. Since at long times the dephasing of the nnn pair is dominated by fluorine noise, the plots with and without ring-exchange (RE) differ very little on a log scale as plotted in the main text. On a linear scale, the difference in the short-time decay becomes apparent. Since for most applications the first $1/e$-decay is the most relevant, the importance of understanding the ring-exchange becomes evident.

---

[6]The reason for this is that the echo decays of loose pairs are dominated by interactions with clock-state ions (and fluorine spins), while magnetized hyperfine states only contribute marginally. Since we assume a linear dependence $W_\Delta \propto x$, the disorder parameter $\alpha(\Delta)$ of clock states is concentration-independent, $\alpha(\Delta) \propto J_\mathrm{typ}/W_\Delta \sim x/x \sim \mathrm{const}$. Thus, the ratio of fluctuation rates $\tau_{-3/2} \propto \exp(-c_1\alpha(\Delta))/c_2$ at $x = 0.01\%$ and $x = 0.1\%$ is also constant. So for any value of c_1, one can find a value of c_2 that returns the 'optimal' $\tau_{-3/2}$ at both concentrations.
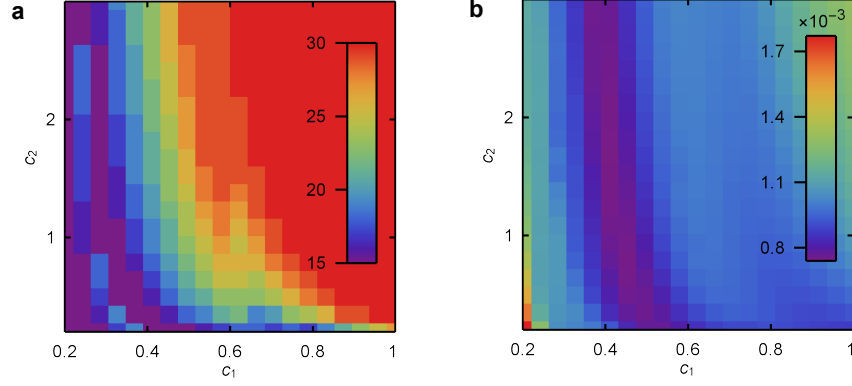
Figure 2: **Results for fit parameters from numerical fit. a** Best fit value of the CF disorder $W_\Delta(x = 0.1\%)$ as a function of c_1 and c_2. **b** Sum of squared residuals of the echo fits as a function of c_1 and c_2.
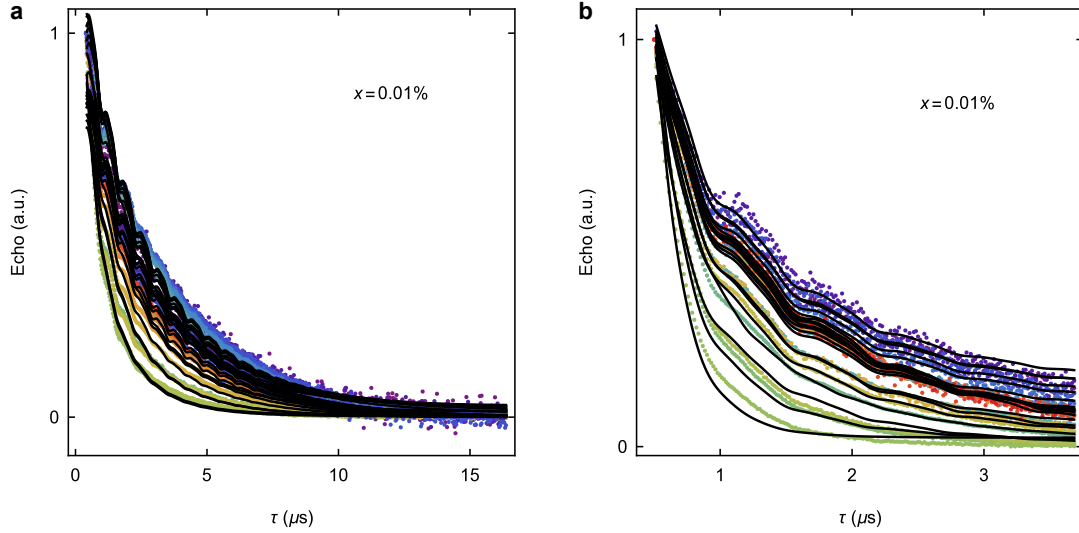

Figure 3: **Hahn-echoes and numerical fits.** Best fit echo traces of loose pairs around $\omega_p = \Delta = 2\pi \times 27.89\,\mathrm{GHz}$ at concentrations of $x = 0.01\%$ (a), and $x = 0.1\%$ (b).
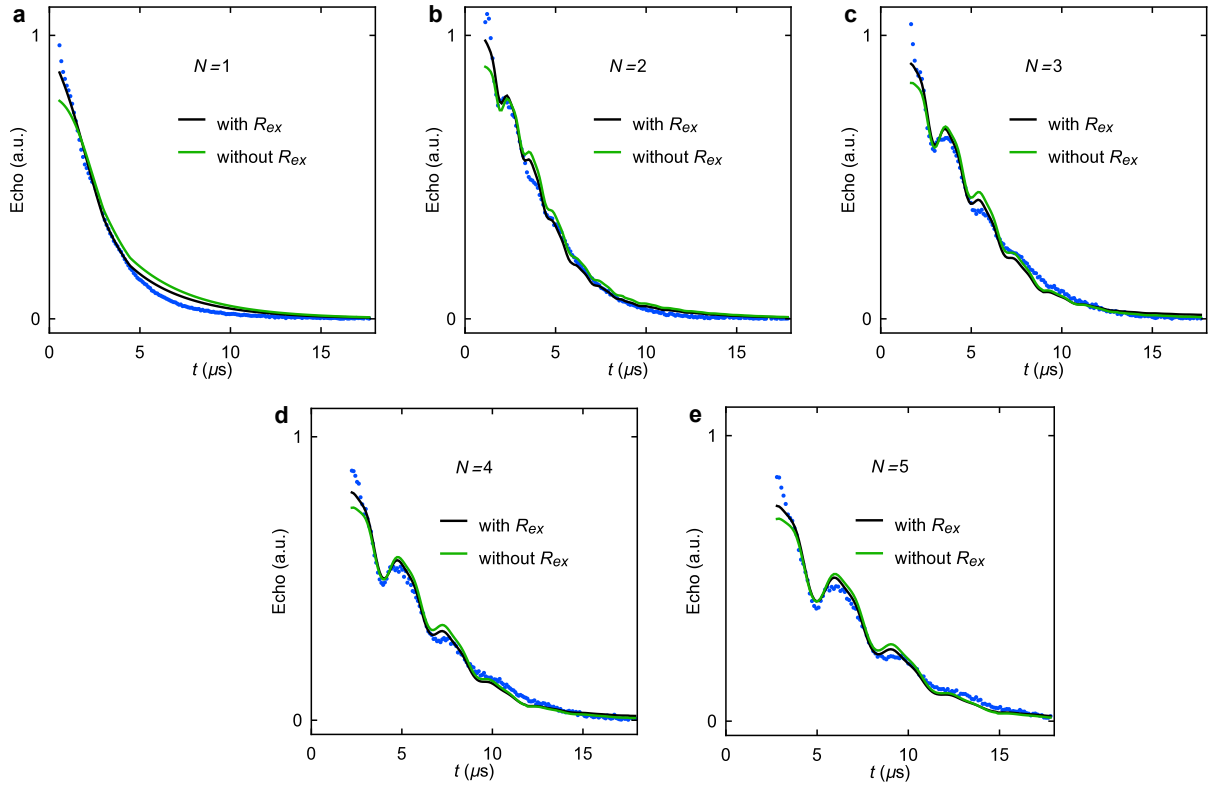
Figure 4: **CPMG echoes and numerical fits.** Echoes of the *nnn* pair under the CPMG protocol, for $N = 1 - 5$ refocusing pulses, at a concentration of $x = 0.1\%$. Fits are shown for the globally best fitting parameters. In green we plot the echo that would be predicted without inclusion of ring-exchange (RE) dephasing, which would lead to a significant slower short-time decay. The amplitudes are adjusted to reduce the sum of squared residuals.

References

[1] A. Beckert, M. Grimm, G. Matmon, N. Wili, R. Tschaggelar, G. Jeschke, S. Gerber, M. Müller, and G. Aeppli, *Emergence of highly coherent quantum subsystems of a noisy and dense spin system*, *Under review at Nature Physics* (2023).

[2] R. Orbach and B. Bleaney, *Spin-lattice relaxation in rare-earth salts*, *Proc. R. Soc. A.*, **264**(1319), 458–484 (1961).

[3] J. Choi, S. Choi, G. Kucsko, P. C. Maurer, B. J. Shields, H. Sumiya, S. Onoda, J. Isoya, E. Demler, F. Jelezko, N. Y. Yao, and M. D. Lukin, *Depolarization dynamics in a strongly interacting solid-state spin ensemble*, *Phys. Rev. Lett.*, **118**, 093601 (2017).

[4] P. Hu and S. R. Hartmann, *Theory of spectral diffusion decay using an uncorrelated-sudden-jump model*, *Phys. Rev. B*, **9**, 1–13 (1974).

[5] J. Bergli, Y. M. Galperin, and B. L. Altshuler, *Decoherence in qubits due to low-frequency noise*, *New J. Phys.*, **11**(2), 025002 (2009).

[6] N. V. Prokof'ev and P. C. E. Stamp, *Theory of the spin bath*, *Rep. Prog. Phys.*, **63**(4), 669–726 (2000).

[7] R. Wannemacher, D. Boye, Y. P. Wang, R. Pradhan, W. Grill, J. E. Rives, and R. S. Meltzer, *Zeeman-switched optical-free-induction decay and dephasing in* $YLiF_4$:Er^{3+}, *Phys. Rev. B*, **40**, 4237–4242 (1989).

[8] N. Kukharchyk, D. Sholokhov, O. Morozov, S. L. Korableva, A. A. Kalachev, and P. A. Bushev, *Optical coherence of* ^{166}Er :$^7LiYF_4$ *crystal below 1 K*, *New J. Phys.*, **20**(2), 023044 (2018).

[9] A. L. Burin and Y. Kagan, *Low-energy collective excitations in glasses. New relaxation mechanism for ultralow temperatures*, *JETP*, **106**, 633–647 (1994).

[10] E. J. Davis, B. Ye, F. Machado, S. A. Meynell, W. Wu, T. Mittiga, W. Schenken, M. Joos, B. Kobrin, Y. Lyu, Z. Wang, D. Bluvstein, S. Choi, C. Zu, A. C. B. Jayich, and N. Y. Yao, *Probing many-body dynamics in a two-dimensional dipolar spin ensemble*, *Nat. Phys.*, **19** 836–844 (2023).

[11] W. M. Witzel and S. D. Sarma, *Multiple-pulse coherence enhancement of solid state spin qubits*, *Phys. Rev. Lett.*, **98**, 077601 (2007).

[12] E. R. Canarie, S. M. Jahn, and S. Stoll, *Quantitative structure-based prediction of electron spin decoherence in organic radicals*, *J. Phys. Chem.*, **11**(9), 3396–3400 (2020).